Stress dependence of magnetization processes: Reversals and relaxation in $Fe_xCo_{85-x}B_{15}$ amorphous ribbons

R. Sato Turtelli,[1,*] J. P. Sinnecker,[2] R. Grössinger,[1] G. Badurek,[3] C. Kussbach,[1] and P. Allia[4]
[1]*Institut für Experimentalphysik, Technische Universität Wien, Wiedner Hauptstrasse 8-10, A-1040, Vienna, Austria*
[2]*Instituto de Física, Universidade Federal do Rio de Janeiro, C. P. 68528, 21945-970 Rio de Janeiro, Brazil*
[3]*Institut für Kernphysik, TU Wien, Stadionallee 2, A-1020, Vienna, Austria*
[4]*Physics Departiment, Politecnico di Torino, Italy*
(Received 14 April 2000; published 13 February 2001)

The effect of stress on the domain-wall dynamics for magnetization reversal and relaxation in $Fe_xCo_{85-x}B_{15}$ amorphous ribbons was investigated by inductance voltage measurements in the absence of applied field after pulse saturating the sample. Optical Kerr-effect and three-dimensional neutron depolarization experiments have been exploited. Residual domains at pinning sites are the main sources of the domains of reversed magnetization. Such a reversal is driven by an internal field through the motion of more than two walls, nucleated at residual domains and/or ribbon edges, and propagating towards the ribbon center. The number of active walls depends on the regularity of the domain structure. An external tensile stress decreases the voltage induced by the change of the magnetization of the sample and delays the ''depinning time t_c'' of the reverse domain walls. A modified Landau-Lifshitz equation was used to interpret the stress dependence of the magnetization reversal and relaxation. We found that t_c is proportional to the coercive field, confirming the validity of the proposed model.

DOI: 10.1103/PhysRevB.63.094427 PACS number(s): 75.60.−d, 75.50.Kj

I. INTRODUCTION

Amorphous $Fe_xCo_{85-x}B_{15}$ ribbons have found wide application in sensor techniques due to their excellent soft magnetic properties. Usually, magnetization reversal in soft magnetic materials takes place by domain wall motion. The rate at which such a reversal occurs depends on the speed of a domain wall and on the number of active domain walls involved in the process. The wall speed is determined by the energy dissipation caused by eddy currents and other relaxation effects. The number of active walls depends mainly on the physical origin of the nucleation of domains with reversed magnetization in the ribbon. It is well known that mechanical stresses in amorphous alloys can significantly affect their soft magnetic properties because of magnetostrictive interactions. However, the stress dependence of domain dynamics and relaxation processes which determine the operation condition of sensor devices have not been clearly established up to now in these materials.

Recently, magnetic relaxation in amorphous ribbons has been studied by means of time-resolved three-dimensional (3D) neutron depolarization after nucleation of a magnetic domain structure in a previously quasisaturated sample, without requiring an ac magnetic field to be applied during the relaxation process.[1] In a magnetostrictive sample exposed to an external stress and for times longer than 10^{-3} s after sudden removal of the external magnetic field, the decay of the magnetic induction with a quasilogarithmic behavior has been interpreted in terms of domain-wall stabilization at the new equilibrium positions. Such a stabilization originates from thermally activated processes of directional ordering of atoms or atomic groups with broadly distributed activation energies.[2–5] However, with this technique, due to the limitations of the experimental setup, investigation of the relaxation phenomenon for times shorter than 10^{-4} s was not possible. Therefore the aim of the present paper is to investigate the domain-wall dynamics for magnetization reversal and relaxation effects that happens at short times in soft magnetic amorphous materials. Additionally, a detailed investigation of the influence of applied tensile stress on domain-wall processes, domain-wall configurations, and propagation of domain walls in amorphous ribbons of the $Fe_xCo_{85-x}B_{15}$ family ($8 \leqslant x \leqslant 85$) is performed. Measurements of the induced voltage on the pickup coils due to the changing magnetization of the sample after impulsive sample saturation are performed in the absence of an applied magnetic field. Domain structures are investigated by means of optical Kerr-effect and three-dimensional neutron depolarization experiments.

II. EXPERIMENTAL PROCEDURE

The voltage induced by the change of the magnetization of amorphous ferromagnetic ribbons after application and removal of a pulsed magnetic field has been measured as a function of time under longitudinal tensile stress σ. Amorphous $Fe_xCo_{85-x}B_{15}$ ribbons ($8 \leqslant x \leqslant 85$) were kindly supplied by the Slovakian Academy of Sciences in Bratislava. The investigations were made at room temperature for as-cast samples and for a single annealed sample of composition $Fe_{64}Co_{21}B_{15}$, heat treated in a furnace at 300 °C for 4 h under 500 MPa. The value of σ was varied from 0 up to around 400 MPa by varying a weight clamped to the lower-lying end of the ribbon. The sample width and length were about 1 and 50 cm, respectively. The thickness, composition, and relevant room-temperature magnetic properties of the examined ribbons are reported in Table I. The $Fe_8Co_{77}B_{15}$ ribbon was found to be partially crystallized, as indicated by x-ray diffraction as well as by its larger coercivity. The co-

TABLE I. Dimensional and room-temperature magnetic parameters of as-cast $Fe_xCo_{85-x}B_{15}$ and Fe-Si–6.5 wt %–Si ribbons.

Sample	l (μm)	λ_s (10^{-6})	I_s (T)	ρ ($\mu\Omega$ cm)	H_c (A/m)
$x=85$	23	36.1	1.53	124	10.7
$x=73$	30	45.5	1.76	118	11.2
$x=64$	28	46.5	1.79	113	10.7
$x=55$	32	41.8	1.75	111	9.3
$x=21$	24	17.8	1.54	96	10.0
$x=8$	19	2.3	1.38	66	19.7
FeSi–6.5 wt %–Si	30	2.5	1.72	82	72.0

ercive force of annealed $Fe_{64}Co_{21}B_{15}$ is about 5 A/m. Similar induced-voltage measurements were also performed for comparison on a rapidly quenched ribbon of microcrystalline FeSi–6.5 wt %–Si in the as-cast condition (see the dimensional and magnetic parameters reported in Table I).

A rectangular-shaped magnetic field pulse of 200 A/m amplitude and a duration of 1 ms and a rise and decay time of 17 μs was periodically applied along the sample with a repetition rate of 2.5 ms by using a coil of 40 cm length. The induced-voltage after completion of the pulse was detected as a function of time by a compensated pickup coil system with 100 turns, would around the sample: the signal was recorded by means of a digital storage oscilloscope. The aftereffect of the initial magnetic permeability was measured by applying a periodic sinusoidal field of 2 A/m amplitude and a frequency of 10 kHz.[6] The saturation magnetostriction λ_s was obtained by means of the small-angle magnetization rotation technique.[7] The coercive force and saturation magnetization were obtained from hysteresis loops measured within a time of 30 s.[8] The demagnetizing field H_d was also estimated from the hysteresis loops; its value is close to the sample coercive field. The changes in the domain structure with both external stress and longitudinal magnetic field were investigated by means of the Kerr-effect technique and 3D static neutron depolarization experiments. For the latter measurements, a crystal polarimeter setup at the 250-kW TRIGA reactor of the Atomic Institute of the University of Technology Vienna was exploited. Setup details and the measurement procedure are described elsewhere.[1]

III. EXPERIMENTAL RESULTS

A. Stress dependence of the domain structure

Kerr images of as-cast state samples reveal a complex fingerprint domain structure [see, e.g., the Kerr image observed on as-cast $Fe_{64}Co_{21}B_{15}$ ribbon shown in Fig. 1(a)]. A regular domain structure is observed in $Fe_xCo_{85-x}B_{15}$ ribbons after annealing or when an external stress σ is applied. Numerous works have been reported about the influence of stress and field annealing on magnetic properties of amorphous ribbons.[9–13] In this work, ribbon with an $x=21$ irregular domain structure is present even after stress annealing, as shown Fig. 2, which contains also domain pattern of stress-annealed $Fe_{73}Co_{12}B_{15}$. The samples were heat treated at 300 °C for 4 h under a tension of 500 MPa.[14] Domain patterns of other magnetostrictive samples are very similar that of $Fe_{73}Co_{12}B_{15}$, which means that the domain structures are regular and the mean number of domains (white and black) lies around 8–10. For the nearly zero-magnetostrictive stress-annealed sample $Fe_8Co_{77}B_{15}$ appears some domains perpendicular to the ribbon axis. A collinear domain alignment with respect to any applied stress has to occur for positive magnetostrictive samples [see Figs. 1(a)–1(f), where the as-cast $Fe_{64}Co_{21}B_{15}$ ribbon was given as an example]. A regular pattern of strip domains indeed starts to develop from about 18 MPa; above 54 MPa, the 180° domain structure is substantially independent of any further increase of σ. This observation is confirmed by Fig. 3, showing the applied stress dependence of the neutron depolarization matrix mea-

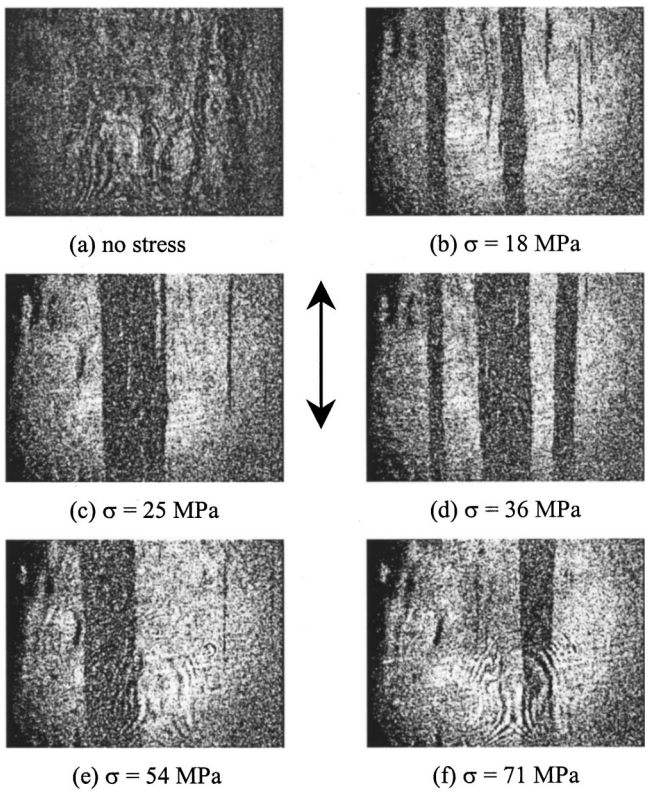

FIG. 1. Kerr-effect images (enlarged scale 13:1) observed on the as-cast $Fe_{64}Co_{21}B_{15}$ ribbon subjected to an increasing applied tensile stress along the axis of ribbon up to 71 MPa. The arrow indicates the direction of the ribbon axis.

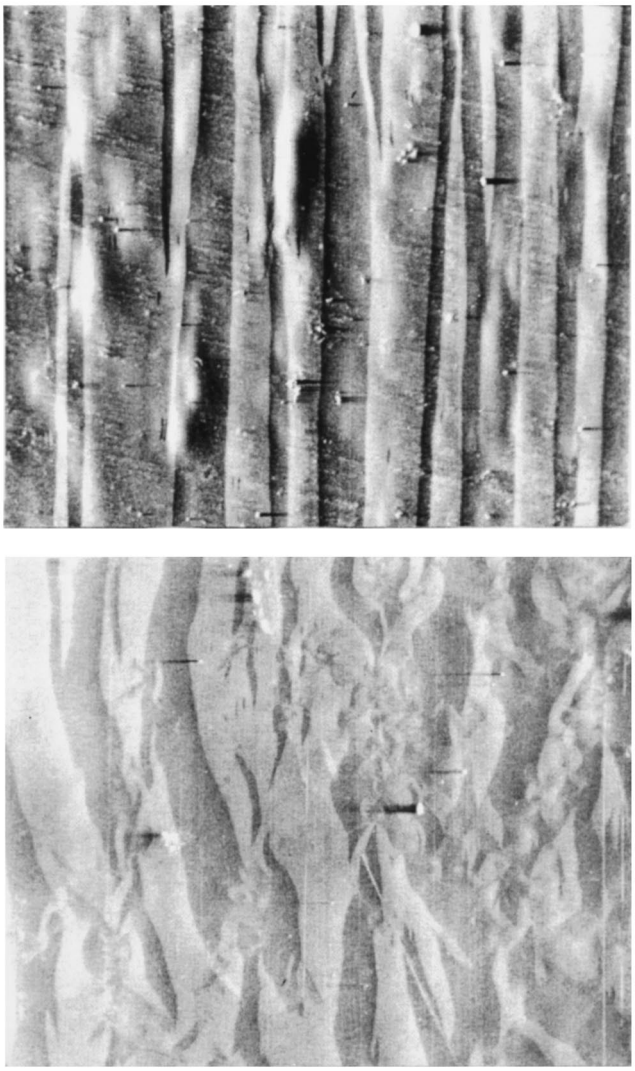

FIG. 2. Domain patterns (enlarged scale 100:1) observed by means of the scanning electron microscopy on the stress-annealed $Fe_{21}Co_{64}B_{15}$ and $Fe_{73}Co_{12}B_{15}$ ribbons (Ref. 14). The arrow shows the direction of the ribbon axis.

sured on $Fe_{85}B_{15}$ and $Fe_{64}Co_{21}B_{15}$ as-cast samples. From the elements of this (3×3) matrix D, which are measured by orienting the polarization vector of the incident neutrons successively in all three directions of space and likewise analyzing all three polarization components after transmission through the sample, averaged domain structure parameters, as mean domain size, mean-square direction cosine of domain magnetization, etc., can be derived.[15] Any variation of domain structure is most sensitively detected from the determinant $|\det D|$ of the depolarization matrix. This determinant is related to the reduced mean magnetization of the sample, and in general it depends in a very complex way upon correlations among neighboring domains. It can be considered as a kind of order parameter reflecting the degree of disorder of the domain structure. For a completely randomized domain arrangement, it tends towards zero with increasing sample thickness, whereas for a fully ordered structure—which causes no depolarization, but only pure spin

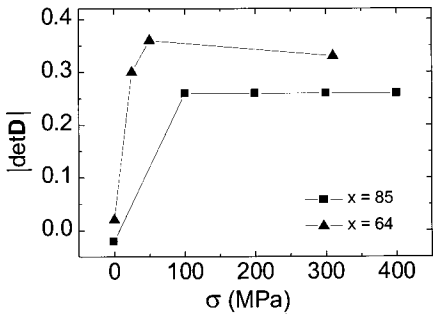

FIG. 3. Determinant of the depolarization matrix as function of the external tensile stress for the as-cast $Fe_{64}Co_{21}B_{15}$ and $Fe_{85}B_{15}$ samples.

rotation—its absolute value approaches 1. It is clearly seen that an external stress causes a significant increase of the related determinant with respect to the unstressed condition, owing to the stress-induced regularity of the domain structure $|\det D|$ increases up to about 50 MPa; for larger values of σ, it remains almost constant.

B. Induced voltage

The oscilloscope trace of the induced voltage in the pickup winding found on as-cast $Fe_{64}Co_{21}B_{15}$ under 31 MPa is given as example of $V(t)$ measurements (see Fig. 4). One can see, indeed, that a nearly complete saturation of the sample's magnetic induction (B_s) is achieved periodically just after the end of the first pulse, as indicated by the fast drop of V, taking a value very close to zero. After completion of the pulse, the curves show a increase of the induced voltage followed by a negative peak V_m occurring at the time referred to as t_c and, subsequently, by a slow decay of the induced voltage. $V(t)$ for different values of the applied stress are shown in Fig. 5, where measurements were performed on annealed $Fe_{64}Co_{21}B_{15}$ and on as-cast $Fe_{21}Co_{64}B_{15}$ and $Fe_8Co_{77}B_{15}$ ribbons. With increasing σ, V_m decreases and t_c is displaced towards larger time values. Similar results were observed in other as-cast samples of the $Fe_xCo_{85-x}B_{15}$ system investigated here. On the other hand, neither the negative peak after the pulse nor the subsequent magnetization decay were observed in the microcrystalline Fe-Si ribbon, both under and without applied stress.

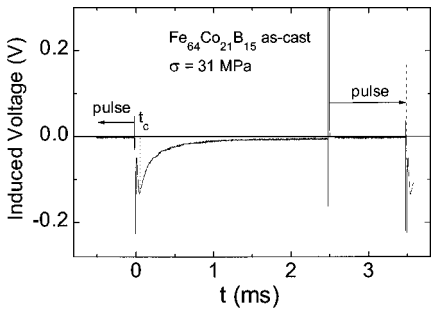

FIG. 4. The induced voltage observed by the oscilloscope for the as-cast $Fe_{64}Co_{21}B_{15}$ ribbon under applied stress of 31 MPa.

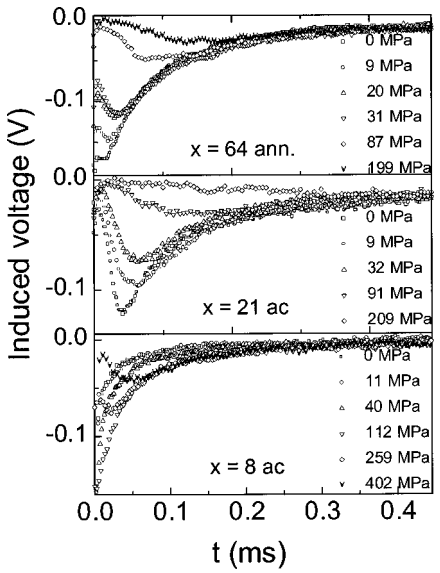

FIG. 5. Time dependence of the induced voltage of as-cast $Fe_8Co_{77}B_{15}$ and $Fe_{21}Co_{64}B_{15}$ alloys and stress-annealed $Fe_{64}Co_{21}B_{15}$ ribbon.

C. Hysteresis loops

Hysteresis loops of $Fe_{64}Co_{21}B_{15}$ ribbons in as-cast and annealed states are shown in Fig. 6. The inset shows the derivative of the magnetization curve of the as-cast sample, exhibiting a peak. The hysteresis loops of stressed ribbons are very similar to that of the annealed sample, showing a quasibistable behavior. With increasing σ, the hysteresis loops become more rectangular shaped.

Figures 7(a)–7(h) show domain configurations observed cycling between positive and negative saturation magnetization (half hysteresis loop) in annealed $Fe_{64}Co_{21}B_{15}$. It is interesting to note the existence of residual domains along the pinning site close to saturation [see Fig. 7(a)]. These residual domains can be the source of an internal field H_r, as will be discussed later. Coming back from saturation to $H = 0.5$ A/m [see Fig. 7(b)], a very small change in the entire domain structure is observed. As the field is reversed, domains grow by the movement of free walls towards the center of the ribbon, leaving stable pinned walls at various pinning sites [indicated by arrows in Fig. 7(c)]. In correspondence to the negative coercivity, the system becomes strongly instable and a Barkhausen jump can occur [see Fig. 7(f)]: a small change in the applied field can cause a big variation in the magnetization, reaching a negative value. Finally Fig. 7(h) shows a domain structure observed at negative saturation, whose configuration, as expected, is just the opposite to that shown in Fig. 7(a) with exactly the same residual domains with reversed spin orientation. Schäfer *et al.*[16] already observed residual domains close to saturation magnetization in amorphous materials.

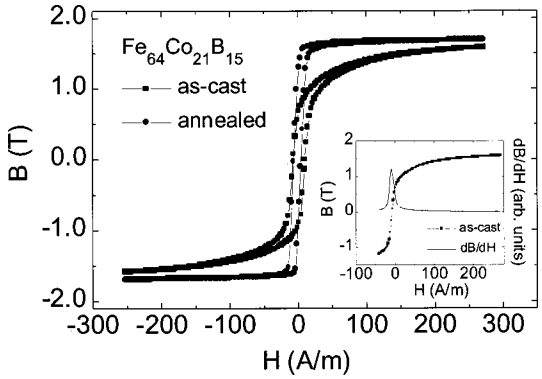

FIG. 6. Hysteresis loops measured on $Fe_{64}Co_{21}B_{15}$ as-cast and annealed samples. The inset shows the derivative of the magnetization curve of the as-cast ribbon.

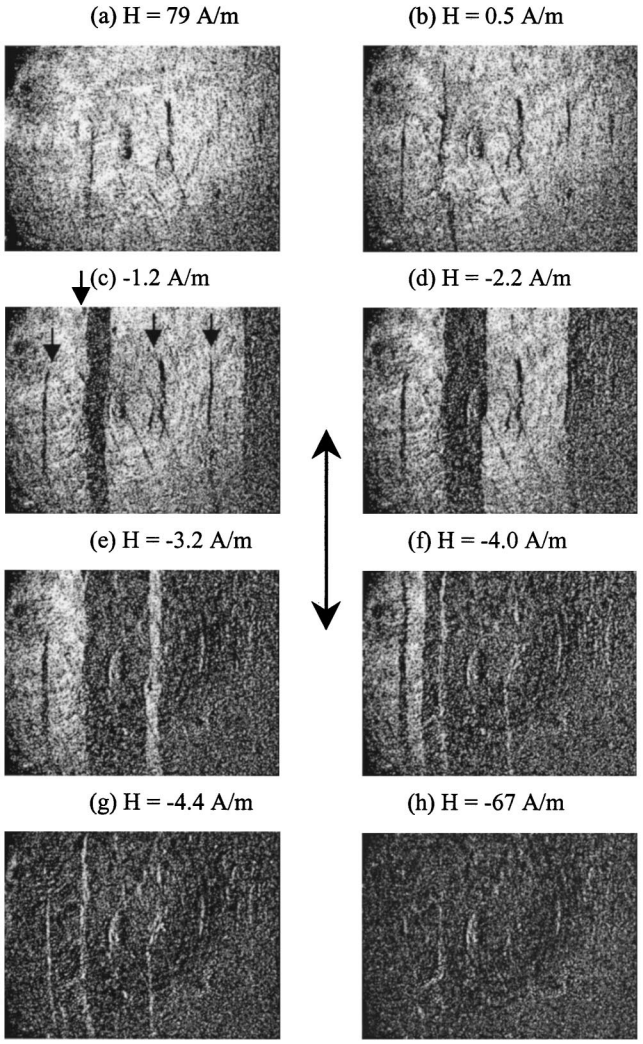

FIG. 7. Kerr-effect images (enlarged scale 13:1) observed on the annealed $Fe_{64}Co_{21}B_{15}$ ribbon cycling between positive and negative saturation magnetization. The dc field was applied along the ribbon axis. A large arrow shows the direction of the applied field and ribbon axis, and small arrows show pinning sites.

D. Time dependence of the magnetization

The observed induced voltage V can be written as

$$V = -N\frac{d\Phi}{dt} = -NA\frac{dB}{dt}, \tag{1}$$

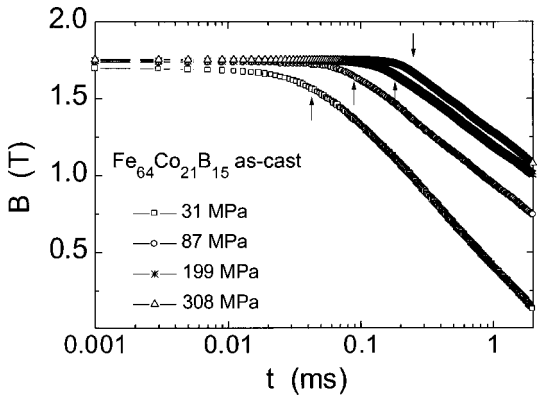

FIG. 8. Magnetic flux obtained from the integral of the induced voltage as function of time for the $Fe_{21}Co_{64}B_{15}$ as-cast ribbon where the parameter is the external tensile stress. Arrows indicate t_c.

where B is magnetic induction, N is the number of turns in a pickup coil, and A is the cross sectional area of the ribbon. As a consequence,

$$\Delta B \cong B_s - B = -\frac{1}{NA}\int V dt, \tag{2}$$

where B_s is the initial (saturation) value. The time behavior of B after completion of the pulse is shown in Fig. 8 (the arrows indicate t_c values) for as-cast $Fe_{64}Co_{21}B_{15}$ under different σ values. After the time t_c the magnetization decays logarithmically with time. In unstressed ribbons ΔB between t_c and 2.5 ms is close to the starting value B_s. Here ΔB decreases with increasing of the applied stress. A similar behavior is observed in all $Fe_xCo_{85-x}B_{15}$ amorphous ribbons.

IV. INTERPRETATION

The observed behavior can be interpreted according to a scheme sketched in Figs. 9(a)–9(e). When the saturating pulse field H_p is applied, the magnetization rapidly jumps to a value close to saturation. In the saturated state the effective internal field of the material, H_i, results from the applied and demagnetizing fields. Figure 9(b), shows the demagnetizing field of the ribbon itself, Hd, and two magnetic poles appearing on residual domain walls, H_r. This residual domains were shown in Fig. 7(a). The value of $H_d + H_r$ is around of the sample coercive field. During the fast decrease of the magnetic field pulse, H_i in turn decreases, reversing during the decay [see Fig. 9(c)] and reaching a value close to H_c. During the pulse drop, a critical field can be reached at which one or more reverse domains can be nucleated. However, close to the critical field each new wall is pinned by local stress and other defects, thus preventing its spontaneous motion. A finite field is needed to overcome such a pinning force. This field, which is a measure of the strength of wall pinning effects, is a threshold field that can be identified as the sample coercive field H_c. However, when pinning effects are particularly strong and the wall energy (per unit surface) is relatively low, as is often the case in amorphous ribbons, a situation may occur where the applied field causes a localized bowing of free segments of the wall between

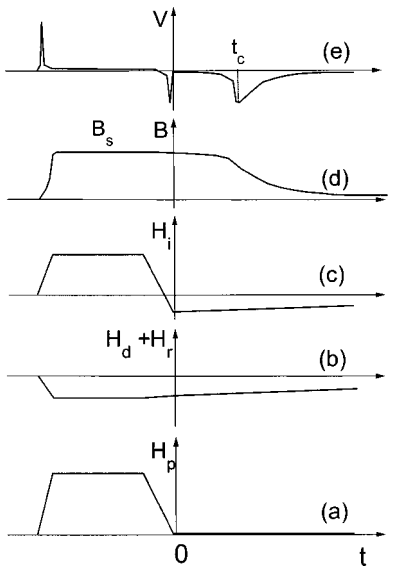

FIG. 9. Scheme of the model: time dependence of the (a) applied pulse field, (b) demagnetizing field composed by the geometrical demagnetizing field, H_d, and that originated by the residual domain, H_r, (c) internal field, (d) magnetization, and (e) induced voltage.

pairs of fixed points (the so-called pinning centers). The bowing starts in correspondence with residual stresses or structurally disordered regions where local residual domains exist. The wall bends, therefore slightly changing the total magnetization. The walls begin to move only when the wall's curvature radius reaches the critical value $r_c = L/2$ (L being the average distance between adjacent pinning centers), collapsing into one or more walls. This occurs at a critical time t_c, and consequently the flattening of the wall surface occurs, reaching an induced voltage V_m. Afterwards, V decreases slowly due to the presence of an energy landscape for the domain walls with a broad distribution of energy barriers. Thus a substantial change of the magnetization can be assumed that starts at t_c. Generally speaking, the coercive field can be viewed as a critical value where any small further increase of the field gives rise to a substantial change of the average wall position, that is, a substantial change of the magnetization of the sample. Therefore, a definite relationship between t_c and the coercive force should exist. This aspect will be discussed in the following section.

V. ANALYSIS OF RESULTS AND DISCUSSION

A. Stress dependence of V_m and t_c

Let us now consider a single 180° domain wall with unit cross sectional area undergoing an induction change ΔB by propagating with velocity v along a distance s in a ribbon of thickness l. From Eq. (1) then follows

$$V = -Nls\frac{dB}{dt} = -\Delta B\, Nlv. \tag{3}$$

If one considers that more than one wall participates in this process and that the number n of effective domain walls can vary, Eq. (1) becomes

$$V = -\Delta B\, nNlv. \tag{4}$$

The presence of more active walls should increase the induced voltage; however, the reversal time is accordingly reduced and therefore the product (voltage×time) remains essentially constant.

On the other hand, the wall speed under the field H_i can be simply obtained from the equation of motion of domain walls:

$$v = \frac{dx}{dt} = \frac{2M_s}{\beta} H_i, \tag{5}$$

where M_s is the saturation magnetization and β is a damping parameter. The ratio $m = 2M_s/\beta$ is the domain-wall mobility. Thus we may rewrite Eq. (4) in the form

$$V = 2M_s nNlH_i \frac{1}{\beta} \Delta B. \tag{6}$$

The damping parameter β measures the energy losses connected with the motion of the domain wall. It has been recognized that it is composed of eddy-current (β_e) and spin-relaxation (β_r) contributions. Generally speaking, the contribution of the first parameter is negligible in soft amorphous ferromagnetic materials. The latter is related to the presence of structural defects which can contribute to the magnetic relaxation mechanism. Before discussing what is the origin of the time dependence of the magnetization, we shall give an equation for V that relates with the applied stress. It is well known that the damping parameter β_r is a characteristic of a particular ferromagnetic domain wall and it relates to parameters which characterize the magnetic material in general such as M_s, the gyromagnetic ratio γ, the anisotropy energy K, and the exchange constant A as is shown in the following relation:[17]

$$\beta_r = \frac{\alpha(1+\alpha^2)M_s}{\gamma} \sqrt{\frac{K}{A}} \cong \frac{\alpha M_s}{\gamma} \sqrt{\frac{K}{A}}. \tag{7}$$

This equation was derived from the Landau-Lifshitz equation with the Gilbert damping coefficient α.[17] Thus β_r varies inversely with the domain wall thickness [$\delta \propto (A/K)^{1/2}$]. One can understand this dependence, considering that for a given domain-wall velocity the spins in a thin wall have to rotate faster than in a broad one. In the case that the stress creates an anisotropy axis along the direction of stress application, the associated anisotropy constant is given by $K = 3\lambda_s \sigma/2$, where λ_s is the saturation magnetostriction. Thus, neglecting the contribution of β_e on the mobility of walls, the stress dependence of V can be given by

$$V = -\frac{2\Delta B\, N\gamma nlH_i \sqrt{2A}}{\alpha\sqrt{3\lambda_s}} \frac{1}{\sqrt{\sigma}}. \tag{8}$$

This equation predicts that in a given material with a 180° domain wall, V varies with $1/\sqrt{\sigma}$. In fact, this relation was experimentally observed for all as-cast ribbons here studied for $\sigma > 10$ MPa as the domain structure becomes regular.

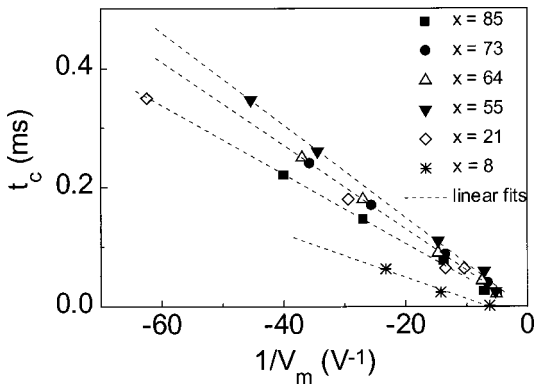

FIG. 10. The time t_c as function of the inverse of V_m for $Fe_xCo_{85-x}B_{15}$ as-cast samples.

Let us now derive a relation that correlates t_c with σ. One can assume that a certain portion of the wall is curved with a velocity v up to the critical radius $r_c = L/2$; then, it is collapsed at t_c. Then the critical radius r_c may be related to t_c by the following relation:

$$t_c = \frac{r_c}{v} = r_c \Delta B\, lNn \frac{1}{V_m} = \frac{\alpha r_c}{2\gamma H_i} \sqrt{\frac{3}{2A}} \sqrt{\lambda_s}\sqrt{\sigma} = C\sqrt{\lambda_s}\sqrt{\sigma}, \tag{9}$$

where $C = \alpha r_c \sqrt{3}/2\gamma H_i \sqrt{2A}$. We found excellent agreement between the experimental data and relation (9). Here t_c as a function of the inverse of V_m and t_c as a function of $\sigma^{1/2}$ investigated for all studied alloy compositions are shown, respectively, in Figs. 10 and 11. For sufficiently small σ, the magnetic reversal and the collapsing of walls occur during the magnetizing field switching process; i.e., the domain wall nucleates and starts to propagate still during the decay of the saturating field pulse. When σ increases, the rate of wall deformation decreases and V_m is observed after the pulse. In Figs. 10 and 11, the dashed lines are obtained by linear fitting. As predicted in Eq. (9), the coefficient of the slope changes according to $\lambda_s^{1/2}$, except for $Fe_{21}Co_{64}B_{15}$, whose t_c value should be smaller than actually observed. Probably this difference originates from a smaller number of active walls than in other samples. As mentioned before and shown in Fig. 2, this particular sample always exhibits an irregular

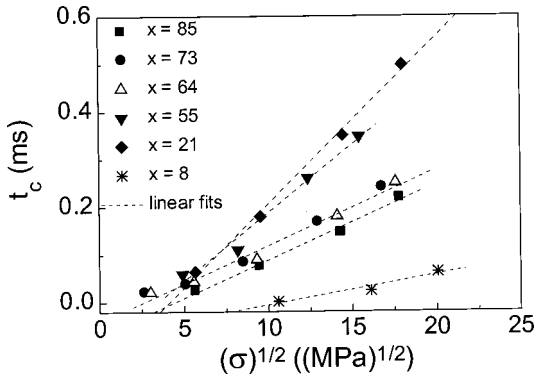

FIG. 11. The time t_c as function of $\sigma^{1/2}$ for $Fe_xCo_{85-x}B_{15}$ as-cast samples.

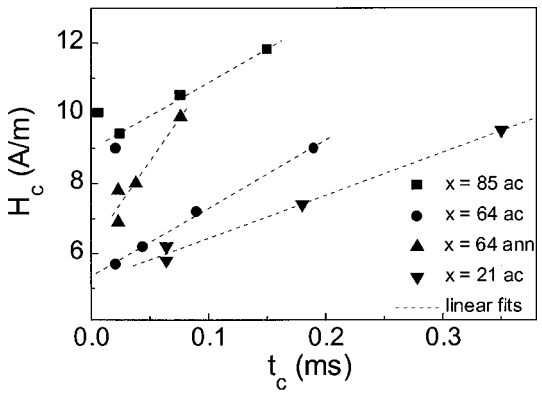

FIG. 12. The coercive force as function as t_c for $Fe_xCo_{85-x}B_{15}$ alloys.

domain structure, which may contribute to a larger number of pinning centers. A decrease in the number of active walls lowers the intensity of the induction voltage and increases t_c.

B. Relation between the coercive force and t_c

If one assumes that a certain bowing condition is a consequence of pinning field and in the energy balance involves both the wall energy $\gamma_w S$ (S is the wall surface) and the field energy $2M_sH_c\Omega$ (Ω is the volume swept by the bowed wall), then the coercive field H_c at the critical value $r_c = L/2$ can be determined as follows:

$$\gamma_w S = 2M_s H_c \Omega, \tag{10}$$

$$H_c = \frac{\gamma_w}{M_s L} = C' \sqrt{\lambda_s}\sqrt{\sigma}, \tag{11}$$

where $\gamma_w = 4(AK)^{1/2}$ and $C' = \sqrt{6A}/r_c M_s$. Comparing Eqs. (9) and (11), the coercive field varies proportionally to t_c. Figure 12 shows H_c as a function of t_c obtained for various samples. Good agreement between the model and experimental data was found. These results again confirm the basic model in which walls are pinned, causing a bowing.

C. Time dependence of the magnetization

A logarithmic time dependence of the magnetization is often observed in soft magnetic amorphous materials. The logarithmic relaxation is due to the presence of a energy landscape E for the domain walls with a broad distribution of energy barriers around a mean value $\overline{E}$. In the presence of diffusion effects, the magnetic aftereffect is originated from the reordering of the structural defects with a time fluctuating energy landscape. Generally, this aftereffect is observed by measuring the time dependence of the initial ac permeability, the disaccommodation.[2–5] On the other hand, in the absence of any diffusion effects, this decline with time must be due to the thermal activation of domains or domain walls, over free energy barriers. Because the domain walls are sensitive to the presence of structural defects and/or disorder, it is reasonable to expect slow relaxation to occur in amorphous materials with or without the presence of a local reordering of atomic groups. Furthermore, both the magnetic relaxation and disaccommodation may be affected by stress in a similar way, because it induces an effective anisotropy that sets the energy of the domain walls [see Eq. (10)] and, therefore, the intensity of the interaction with the pinning centers.

TABLE II. Values of aftereffect of the initial permeability measured between 4 ms and 4 s and relaxation magnetization taken between 0.1 and 2.5 ms after completion of the saturating pulse obtained for $Fe_xCo_{85-x}B_{15}$ as-cast ribbons.

Sample	$\Delta B\,H/B$ (A/m)	ΔB (T)
$x=85$	0.16	0.61
$x=73$	0.32	1.44
$x=64$	0.32	1.32
$x=55$	0.30	1.25
$x=21$	0.19	0.71
$x=8$	0.12	0.40

To have a comparison, in Table II values of the magnetic relaxation taken between 0.1 and 2.5 ms after completion of the saturating pulse and the disaccommodation, $\Delta B\,H/B$, measured between 4 ms and 4 s measured on unstressed ribbons at room temperature, are given. The relation between them is constant and lies around 4. The stress dependence of the magnetic relaxation is shown in Fig. 13. The intensity of the magnetic relaxation observed at short times tends to increase with increasing applied stress, owing to compensation of the internal stress then, it decreases with further increase of σ. For the sample ($x=8$) exhibiting the lowest magnetostriction, the value $\Delta B(\sigma)$ increases up to $\sigma = 120$ MPa; then, it decreases again. A similar behavior was observed by Allia *et al.* in their investigation of the stress dependence of the initial susceptibility.[18]

The short-time magnetic relaxation is not observed in the FeSi–6.5 wt %–Si microcrystalline ribbon. In the microcrystalline alloy, magnetization reversal necessarily occurs during the decay of the saturating pulse, and hence the fast damping of nucleated domain walls is attributable to a comparatively larger effect of eddy currents.

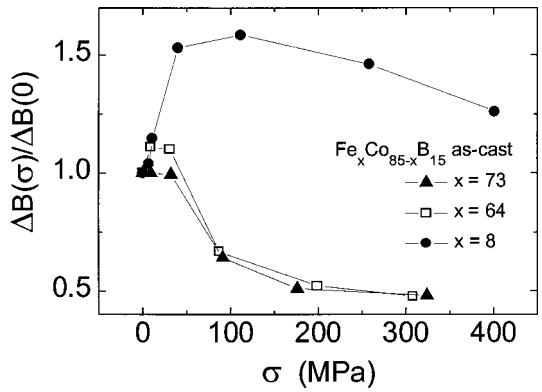

FIG. 13. External tensile stress dependence of the aftereffect of the magnetization observed on $Fe_{73}Co_{12}B_{15}$, $Fe_{64}Co_{21}B_{15}$, and $Fe_8Co_{77}B_{15}$ as-cast ribbons.

VI. CONCLUSION

A detail investigation of the dynamic magnetization process for $10^{-5}<t<10^{-3}$ was performed measuring the induced voltage on the pickup coils due to the changing magnetization of the sample after sample pulsed saturation. The reverse domain proceeded by the action of an internal field (originating from the demagnetizing field and residual domains at the pinning sites) through the motion of more than two walls. The number of active walls depends on the regularity of the domain structure. An external stress decreases the induced voltage, the intensity of the magnetization relaxation, and delays the collapsing of reverse domains from pinning centers after sample pulsed saturation. It was concluded that the coercive force is proportional to t_c, confirming thus the validity of the proposed model.

ACKNOWLEDGMENTS

This work was partly supported by KELAG. The authors thank Dr. C. Beatrice of the Instituto Electtrotecnico Nazionale ''Galileo Ferraris,'' Torino, Italy, for the facilities to use the optical Kerr-effect system.

*Corresponding author Fax: +43-1-58801-13199. Electronic address: sato@xphys.tuwien.ac.at

[1] J. P. Sinnecker, R. Sato Turtelli, R. Grössinger, G. Badurek, P. Riedler, and S. Menhart, J. Appl. Phys. **85**, 1043 (1999).
[2] H. Kronmüller, Philos. Mag. B **48**, 127 (1983).
[3] P. Allia and F. Vinai, Phys. Rev. B **33**, 422 (1986).
[4] C. Kussbach, R. Sato Turtelli, C. Kuss, D. Holzer, and R. Grössinger, J. Magn. Magn. Mater. **160**, 293 (1996).
[5] R. Sato Turtelli, R. Grössinger, C. Kussbach, and J. P. Sinnecker, J. Appl. Phys. **83**, 1581 (1998).
[6] J. P. Sinnecker, Ph.D. thesis, Institute of Physics, University of Campinas, Brasil, 1997.
[7] K. Narita, J. Yamasaki, and H. Fukunaga, IEEE Trans. Magn. **16**, 435 (1980).
[8] D. Holzer, Ph.D. thesis, Institute of Experimental Physics, University of Vienna, Austria, 1998.
[9] O. V. Nielsen, J. M. Barandiaran, A. Hernando, and V. Madurga, J. Magn. Magn. Mater. **49**, 124 (1985).
[10] J. M. Barandiaran, A. Hernando, V. Madruga, O. V. Nielsen, M. Vazquez, and M. Vazquez-Lopez, Phys. Rev. B **35**, 5066 (1987).
[11] A. Hernando, M. Vazquez, G. Rivero, and J. M. Barandiaran, J. Magn. Magn. Mater. **101**, 6 (1991).
[12] A. Siemko, H. K. Lachowicz, and A. Slawska-Waniewska, J. Magn. Magn. Mater. **101**, 16 (1991).
[13] E. Wittig, R. Grossinger, R. Sato Turtelli, and C. Kussbach, Mater. Sci. Forum **235-238**, 691 (1997).
[14] K. Záveta (unpublished).
[15] R. Rosman and M. Th. Rekveldt, Phys. Rev. B **43**, 8437 (1991).
[16] R. Schäfer, W. K. Ho, J. Yamasaki, A. Hubert, and F. B. Humphrey, IEEE Trans. Magn. **MAG-27**, 3678 (1991).
[17] R. C. O'Handley, J. Appl. Phys. **46**, 4996 (1975).
[18] P. Allia, C. Beatrice, and F. Vinai, IEEE Trans. Magn. **MAG-22**, 430 (1996).